

Lithium confinement and dynamics in hexagonal and monoclinic tungsten oxide nanocrystals: ^{7}Li solid state NMR study

René Dören^a, Martin Panthöfer^a, Leon Prädel^b, Wolfgang Tremel^{a,*} and Mihail Mondeshki^{a,*}

^aDepartment Chemie, Johannes Gutenberg-Universität, Duesbergweg 10-14, D-55128 Mainz, Germany

^bMax Planck Institute for Polymer Research, Ackermannweg 10, 55128 Mainz, Germany

Table S1. Fit data for deconvoluted ¹H-MAS-NMR spectra.

| Sample | Position / ppm | Intensity a.u. | Area a.u. | FWHM / Hz | Ratio L/G | gof ^a |
|-------------|----------------|----------------|-----------|-----------|-----------|------------------|
| h-LiATB@RT | 6.83 | 58.56 | 107.70 | 590.27 | 0.00 | 99.9 % |
| | 5.25 | 319.99 | 655.59 | 629.52 | 0.40 | |
| | 2.13 | 45.44 | 158.08 | 1153.27 | 0.20 | |
| | 0.91 | 120.46 | 217.60 | 580.93 | 0.01 | |
| h-LiATB@300 | 6.64 | 181.96 | 225.38 | 342.91 | 0.89 | 98.0 % |
| | 3.69 | 17.73 | 41.66 | 750.00 | 0.08 | |
| | 0.99 | 1.55 | 1.96 | 398.39 | 0.00 | |
| m-LiTb@500 | 4.28 | 88.25 | 166.80 | 594.00 | 0.10 | 92.6 % |
| | 1.11 | 4.10 | 2.98 | 224.00 | 0.00 | |

a. Overlap of fit profile and real spectra

Table S2. Fit data for deconvoluted ^{7}Li -MAS-NMR spectra.

| Sample | Position / ppm | Intensity a.u. | Area a.u. | FWHM / Hz | Ratio L/G | gof ^a |
|-------------|----------------|----------------|-----------|-----------|-----------|------------------|
| h-LiATB@RT | -0.46 | 1204.31 | 2861.52 | 263.38 | 1.00 | 85 % |
| | -2.18 | 757.01 | 2041.71 | 315.60 | 1.00 | |
| h-LiATB@300 | -0.36 | 1140.38 | 3199.60 | 330.90 | 0.82 | 92 % |
| | -2.41 | 563.36 | 1190.91 | 258.50 | 0.54 | |
| m-LiTb@500 | -0.45 | 327.40 | 830.93 | 283.93 | 1.00 | 91 % |
| | -1.44 | 261.98 | 788.98 | 351.88 | 1.00 | |
| | -2.20 | 371.64 | 908.90 | 314.57 | 0.12 | |

a. Overlap of fit profile and real spectra

$$V(x) = u * L(x) + (u - 1) * G(x)$$

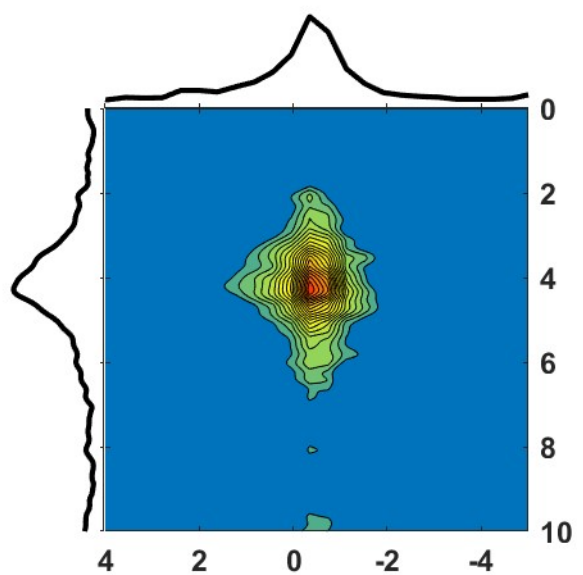


Fig. S1. HETCOR experiment of m-LiT@500 with $t_{CP} = 1$ ms.

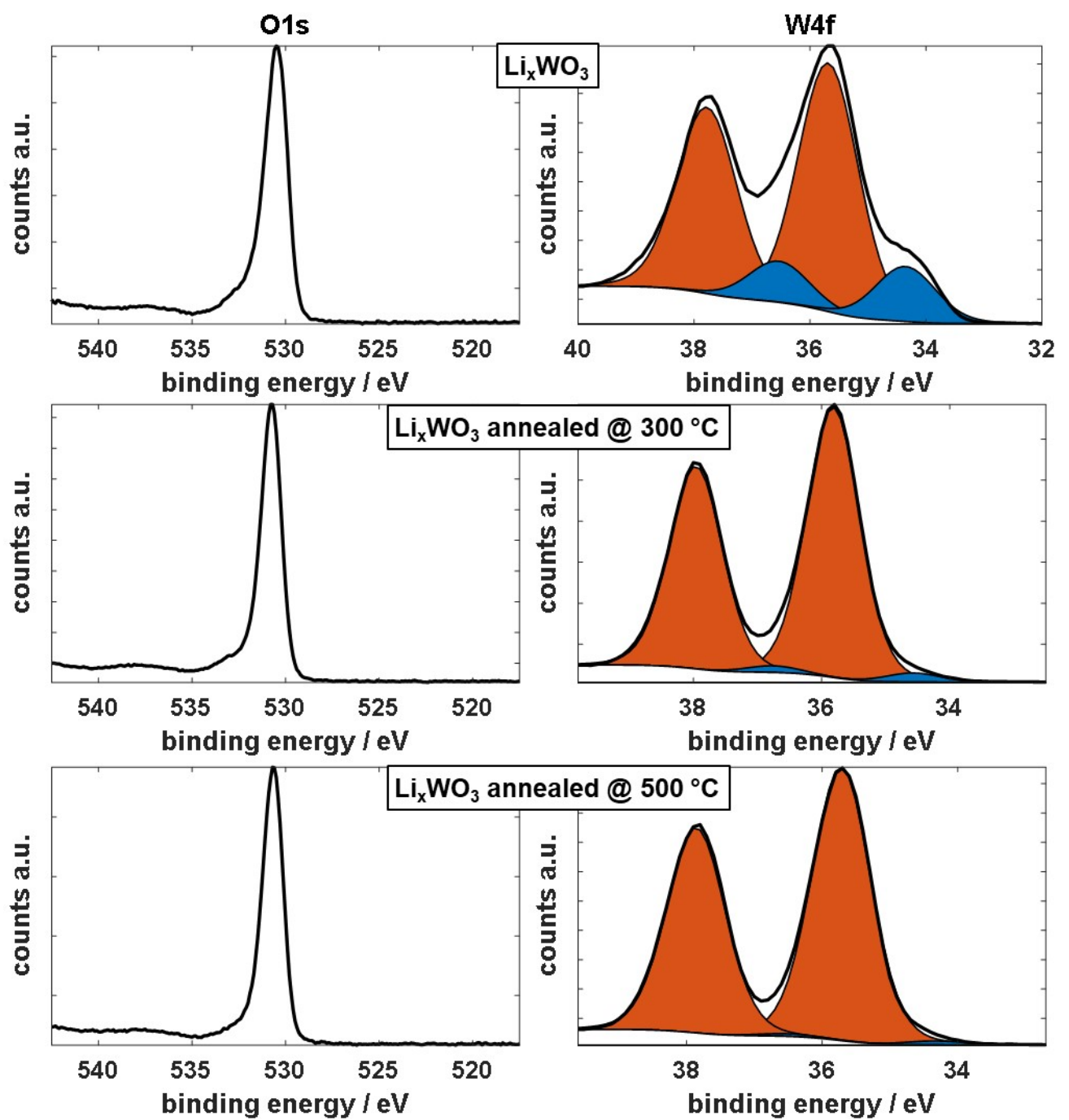


Fig. S2. XPS spectra for O1s and W4f of Li_xWO_3 nanocrystals; not annealed (top), annealed at 300 °C (middle) and annealed at 500 °C (bottom).

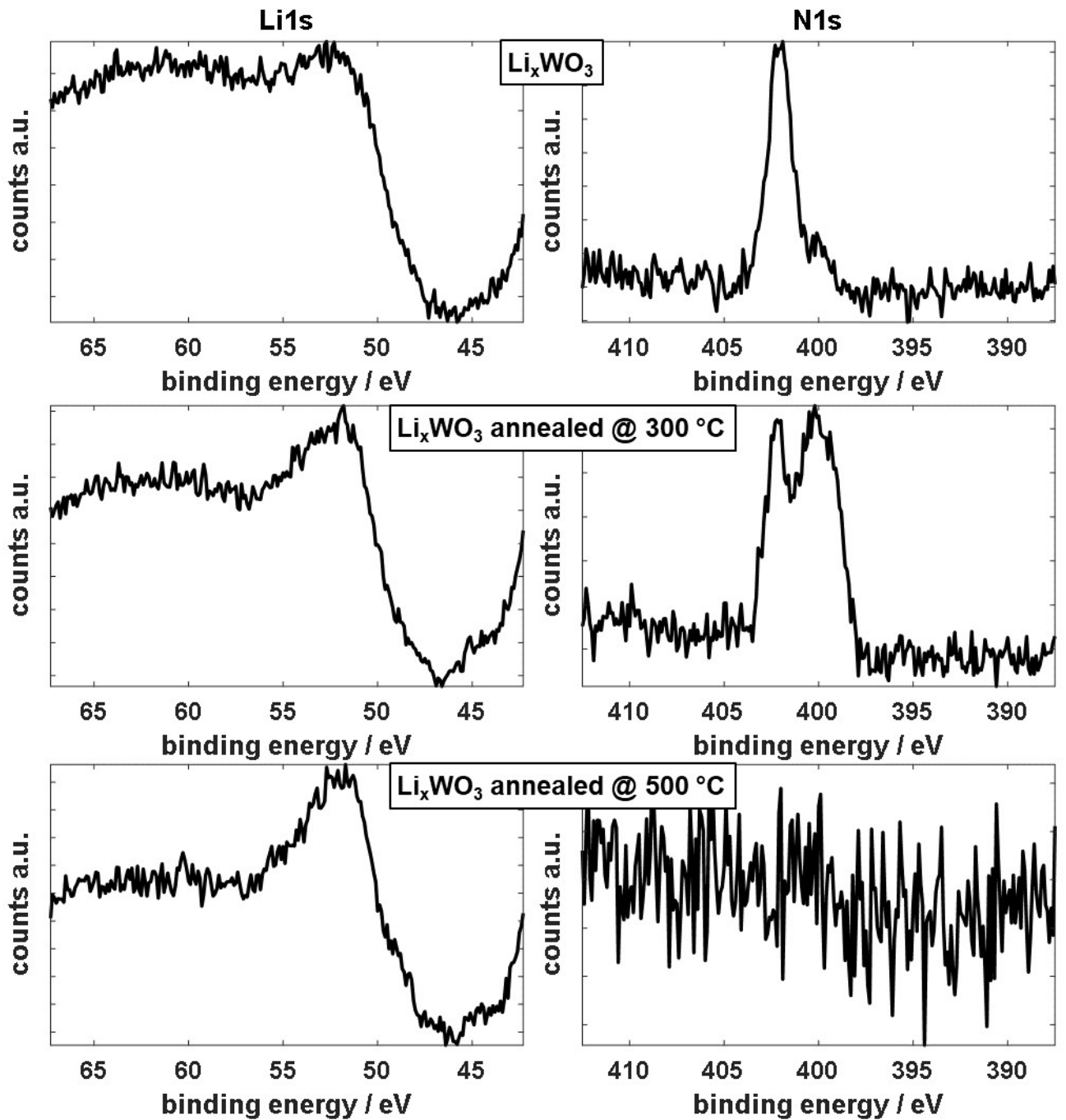


Fig. S3. XPS spectra for Li1s and N1s of Li_xWO_3 nanocrystals; not annealed (top), annealed at 300 °C (middle) and annealed at 500 °C (bottom).

Table S3. T_1 data for the separate signals of h-LiATB@RT, h-LiATB@300 and m-LiT@500 measured at RT, 40 °C and 60 °C, as well as activation energy.

| sample | Shift / ppm | T_1 / s (RT) | T_1 / s (40 °C) | T_1 / s (60 °C) | E_A / kJ/mol |
|-------------|-------------|----------------|-------------------|-------------------|----------------|
| h-LiATB@RT | -0.46 | 0.60 | 0.48 | 0.40 | 8.27 |
| | -2.20 | 6.25 | 5.85 | 3.44 | 11.90 |
| h-LiATB@300 | -0.36 | 3.07 | 2.41 | 1.89 | 11.09 |
| | -2.44 | 14.95 | 14.26 | 12.85 | 3.47 |
| m-LiT@500 | -0.45 | 2.38 | 2.06 | 1.77 | 6.73 |
| | -1.44 | 6.82 | 5.79 | 4.85 | 7.75 |
| | -2.20 | 4.79 | 4.28 | 3.54 | 6.89 |

Table S4. T₂ data for the separate signals of h-LiATB@RT, h-LiATB@300 and m-LiT@500 measured at RT, 40 °C and 60 °C.

| sample | Shift / ppm | T ₂ / ms (RT) | T ₂ / ms (40 °C) | T ₂ / ms (60 °C) |
|-------------|-------------|--------------------------|-----------------------------|-----------------------------|
| h-LiATB@RT | -0.46 | 2.04 | 2.32 | 2.65 |
| | -2.20 | 5.50 | 6.14 | 5.75 |
| h-LiATB@300 | -0.36 | 2.36 | 2.51 | 2.57 |
| | -2.44 | 3.54 | 3.38 | 3.48 |
| m-LiT@500 | -0.45 | 1.60 | 1.63 | 1.84 |
| | -1.44 | 0.64 | 0.56 | 0.58 |
| | -2.20 | 0.79 | 0.91 | 0.88 |

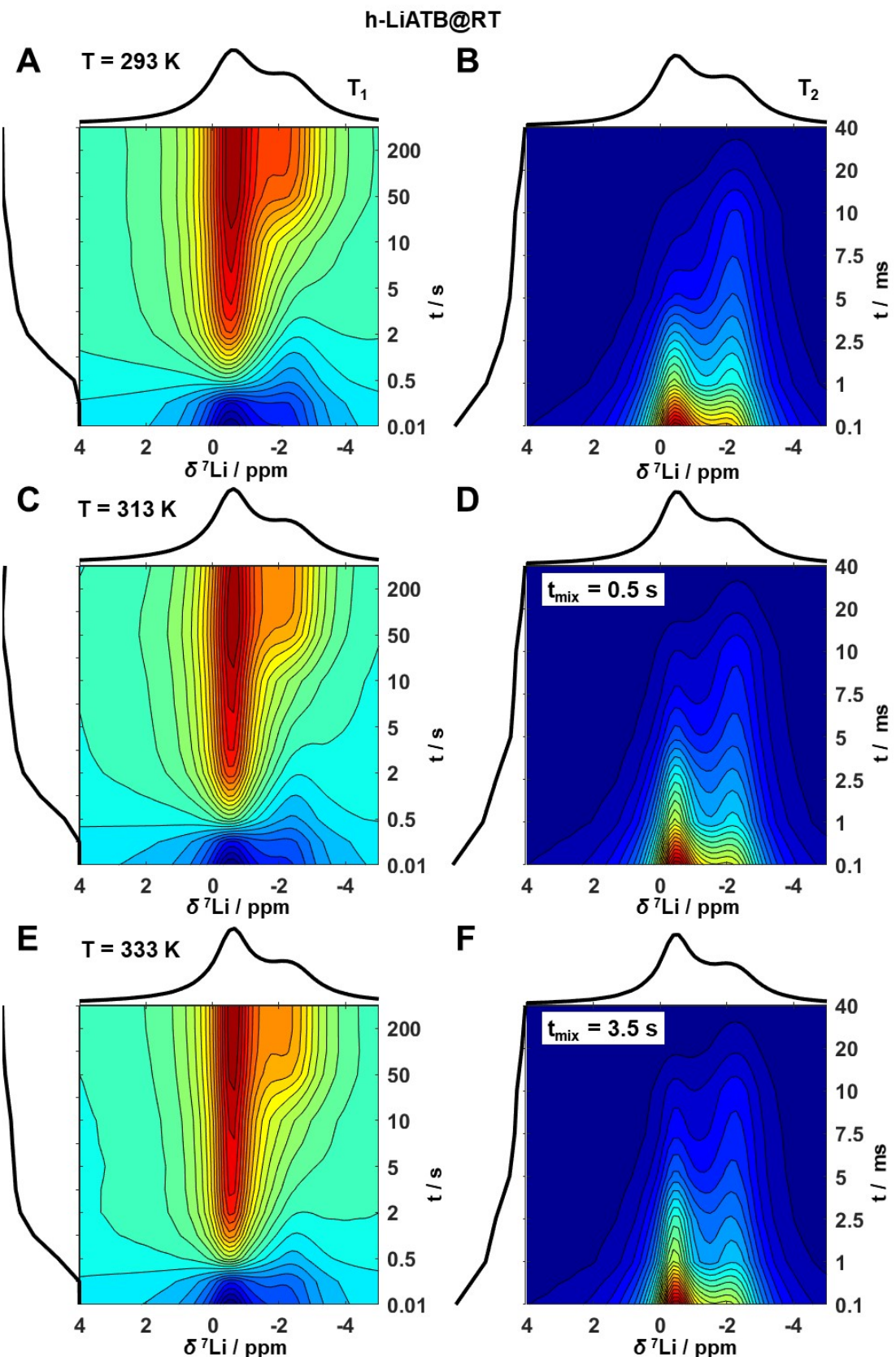


Fig. S4. T_1 (A, C, D) and T_2 (B, D, F) contour plots of h-LiATB@300 measured at RT (A & B), at 40 °C (C & D) and at 60 °C (E & F)

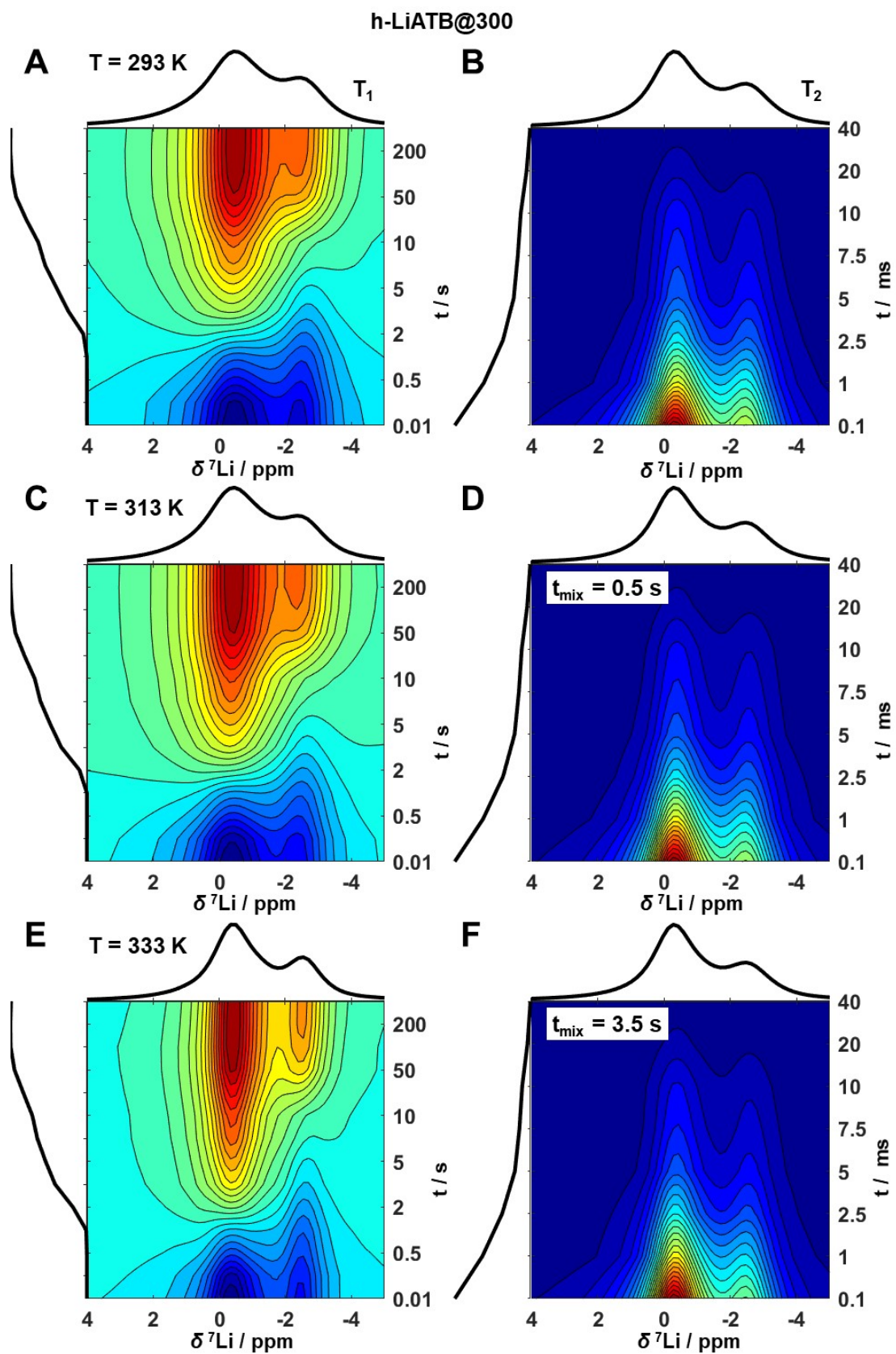


Fig. S

5. T_1 (A, C, D) and T_2 (B, D, F) contour plots of h-LiATB@300 measured at RT (A & B), at 40 °C (C & D) and at 60 °C (E & F)

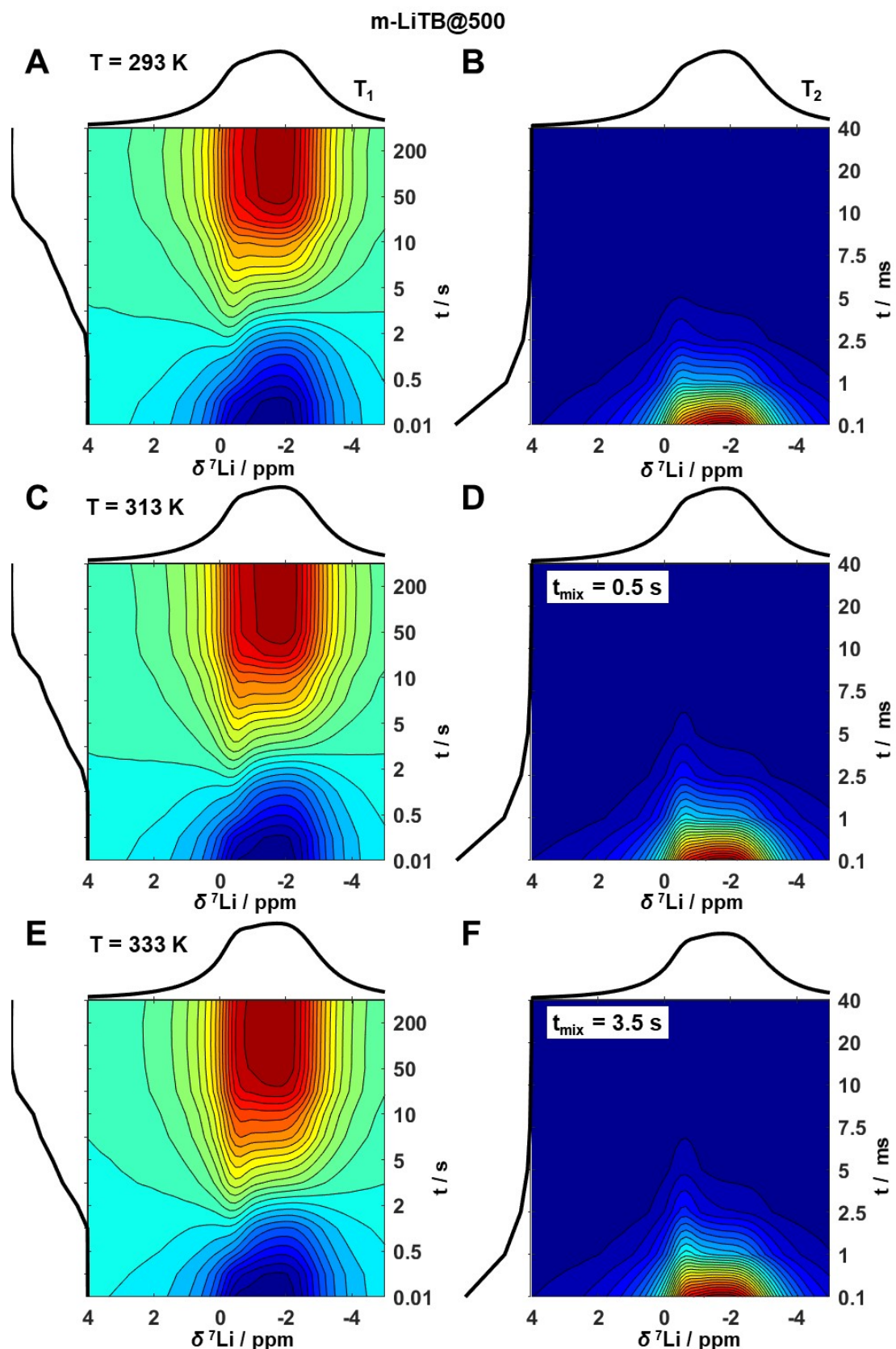


Fig. S6. T_1 (A, C, D) and T_2 (B, D, F) contour plots of h-LiT@300 measured at RT (A & B), at 40 °C (C & D) and at 60 °C (E & F)

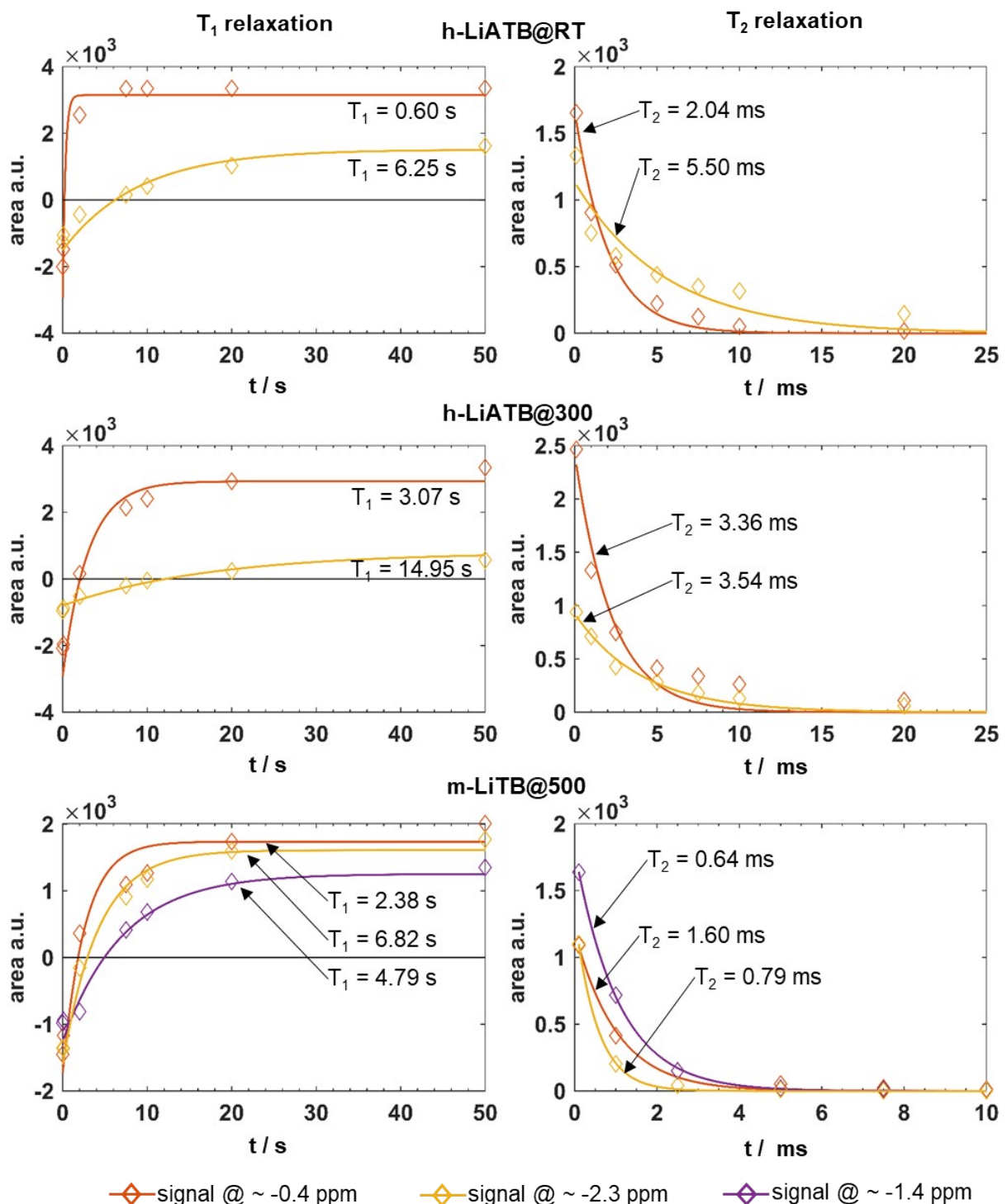


Fig. S7. T_1 and T_2 Fit curves for samples h-LiT@TB@RT (top), h-LiT@TB@300 (middle) and m-LiT@500 (bottom) measured at RT.

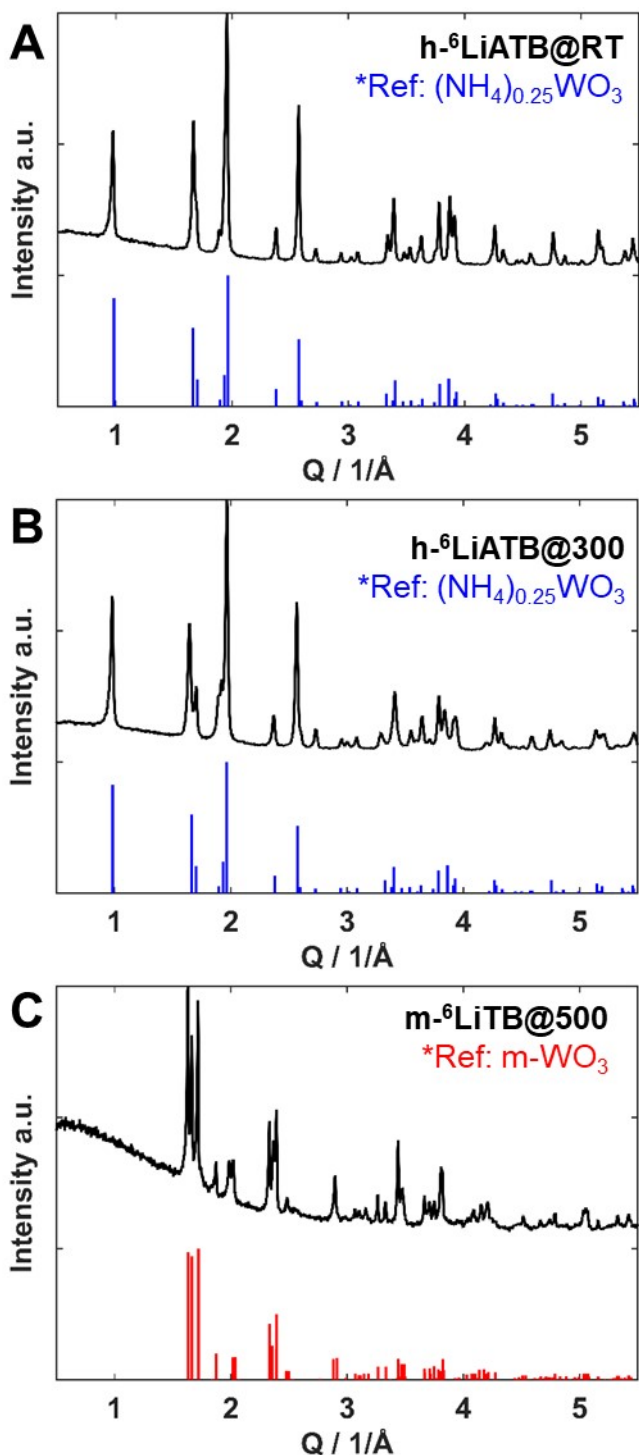


Fig. S8. PXRD patterns of (a) sample A-500 with references for monoclinic WO_3 (space group $\text{P}12_1/\text{n}1$, ICSD no. 99-500-3824), trigonal Li_2WO_4 and (space group $R\bar{3}$, ICSD no. 99-500-4151) and triclinic $\text{Li}_2\text{W}_2\text{O}_7$ and (space group $P\bar{1}$, ICSD no. 99-500-1186).and (b) sample A-300W with references for hexagonal WO_3 (space group $\text{P}6_3/\text{mc}m$, ICSD no. 99-503-1860) and trigonal Li_2WO_4 and (space group $R\bar{3}$, ICSD no. 99-500-4151).

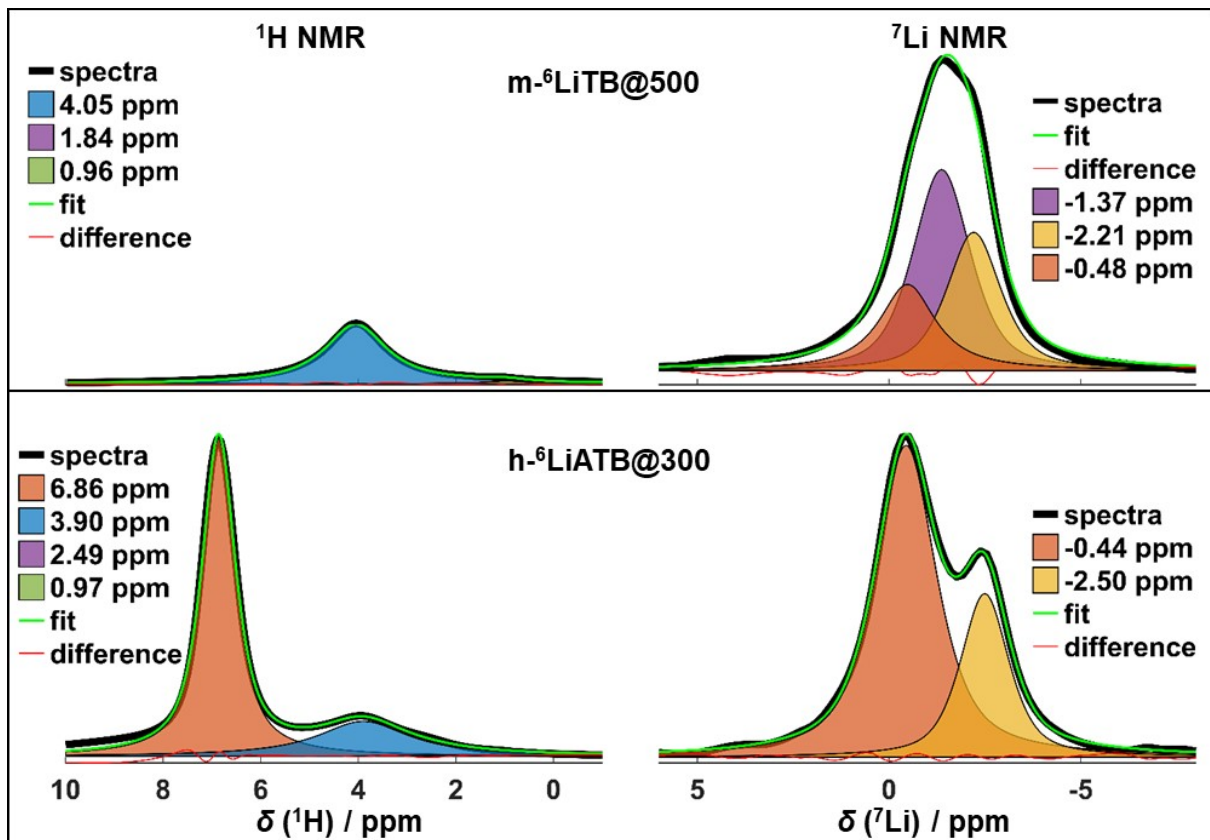


Fig. S9. Solid state MAS-NMR spectra (¹H, right and ⁷Li, left) of (a) and (b) sample B, (c) and (d) sample C-300, (e) and (f) sample C-500. Peaks fitted by pseudo-Voigt profile.

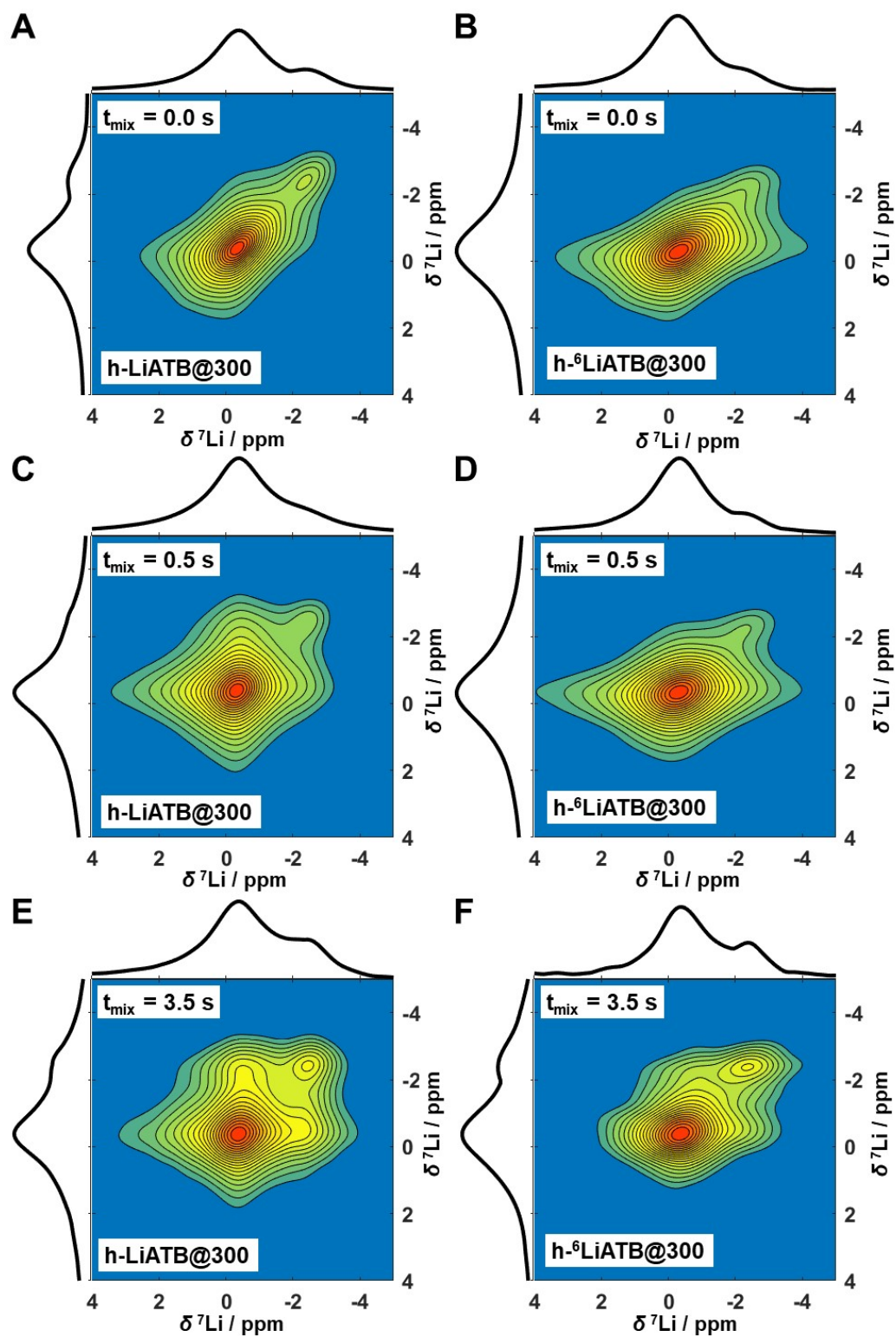


Fig. S10. EXSY spectra of h-LiATB@300 (A, C, E) and h- ^6Li ATB@300 (B, D, F) with mixing times of 0.0 s (A & B), 0.5 s (C & D) and 3.5 s (E & F).

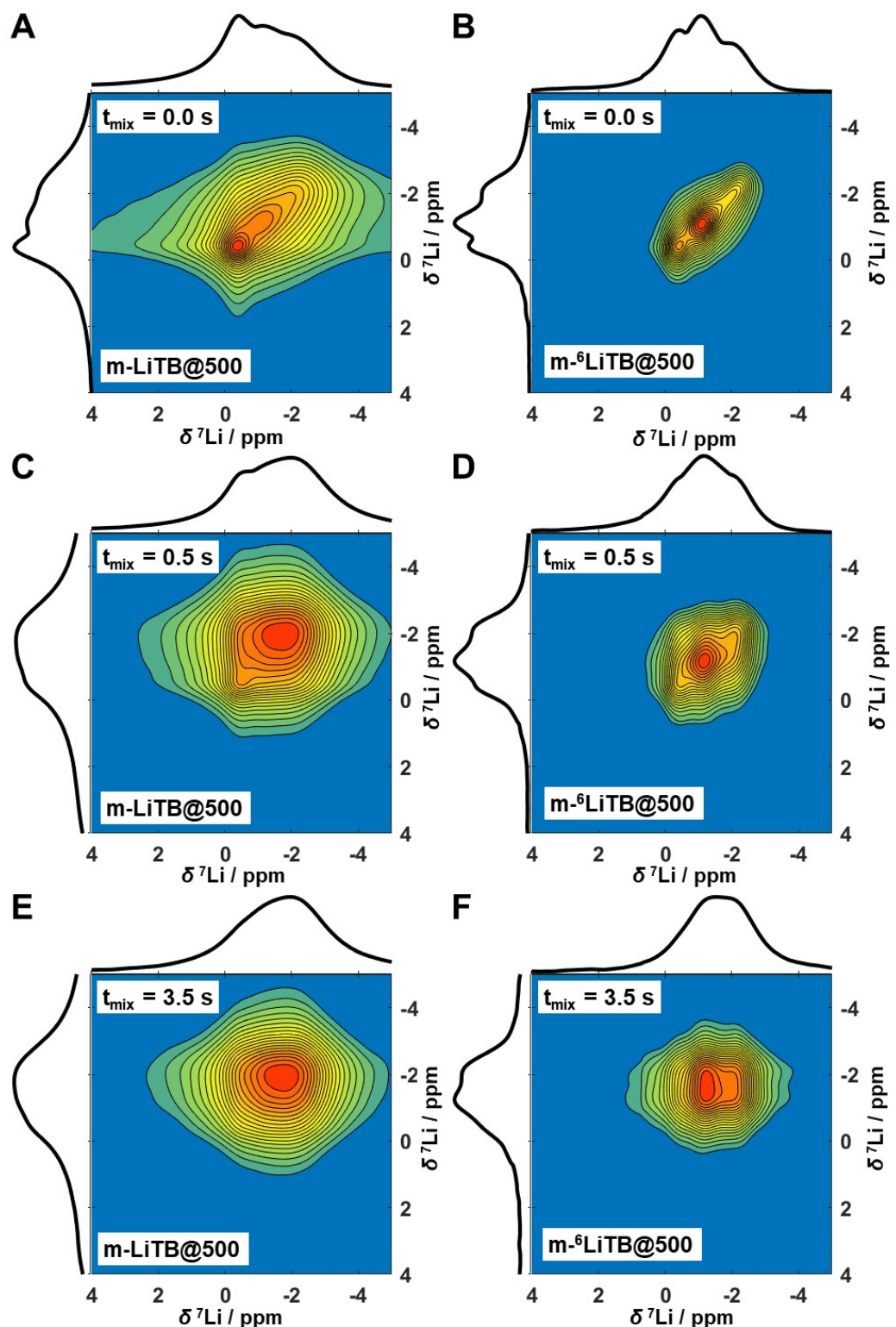


Fig. S11. EXSY spectra of m-LiT@500 (A, C, E) and m-⁶LiT@500 (B, D, F) with mixing times of 0.0 s (A & B), 0.5 s (C & D) and 3.5 s (E & F).

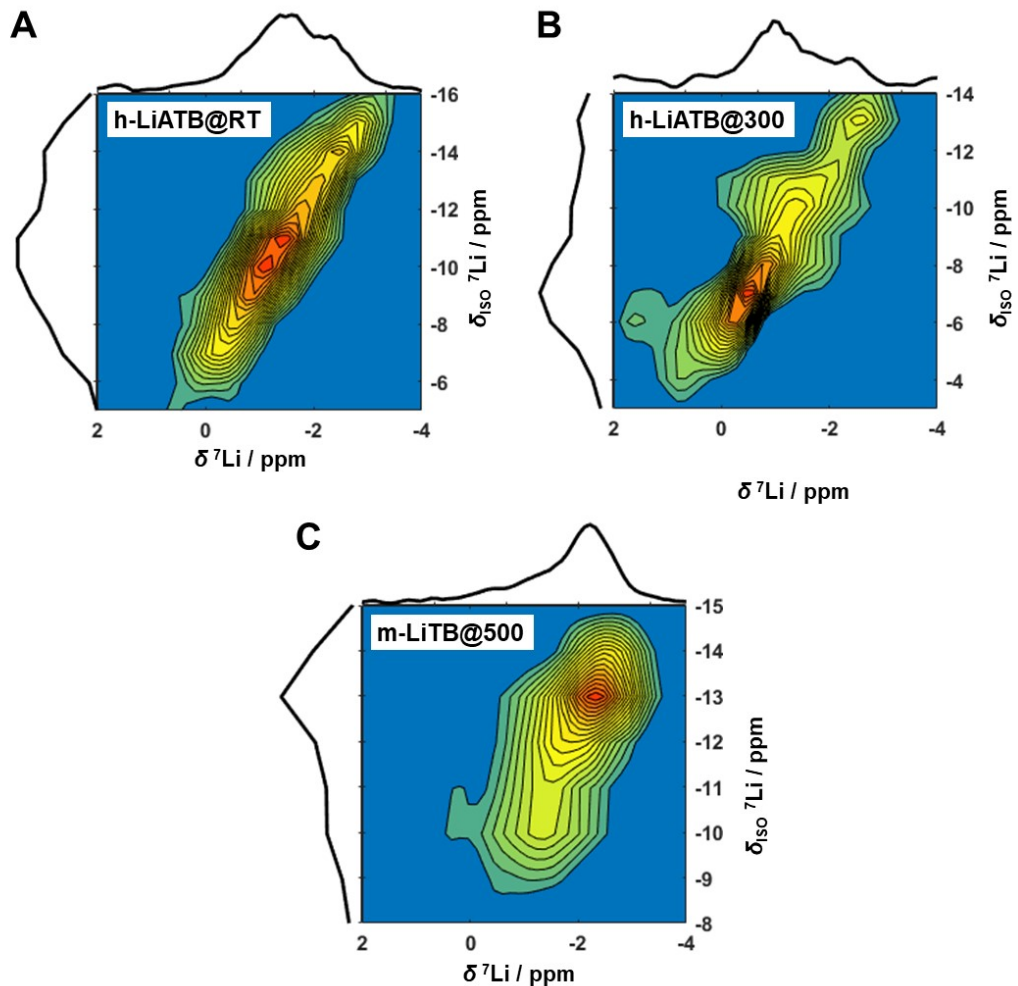


Fig. S12. Unsheared ^7Li MQMAS spectra of h-LiT@RT, h-LiT@300 and m-LiT@500 samples.

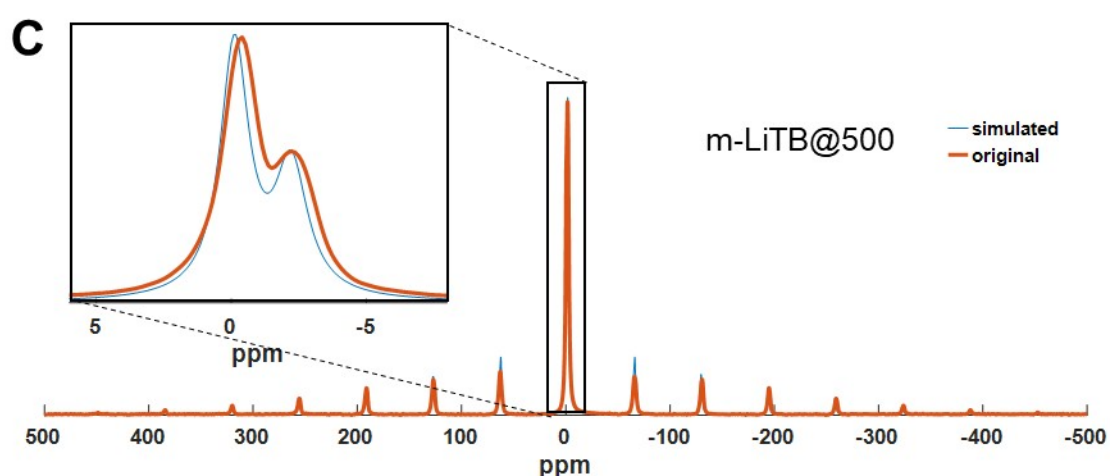
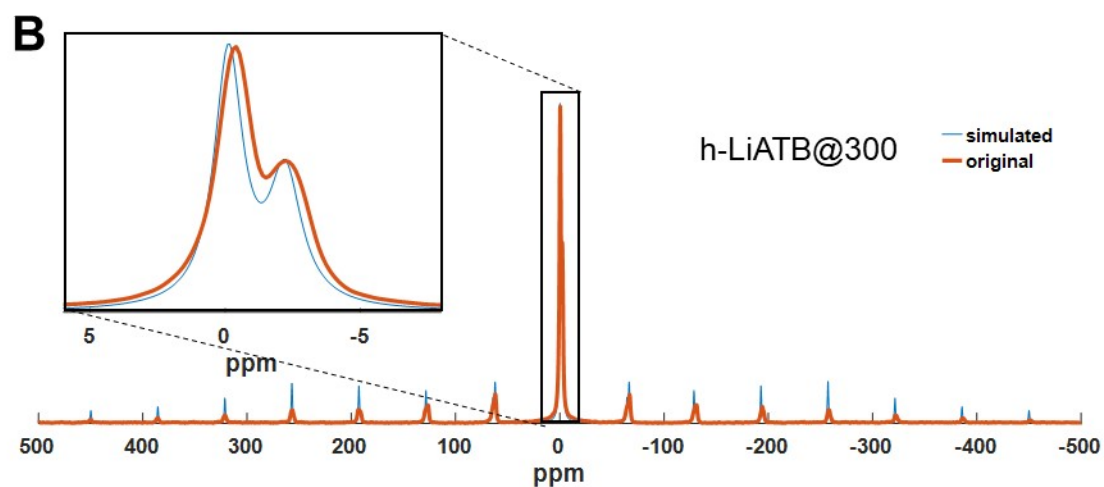
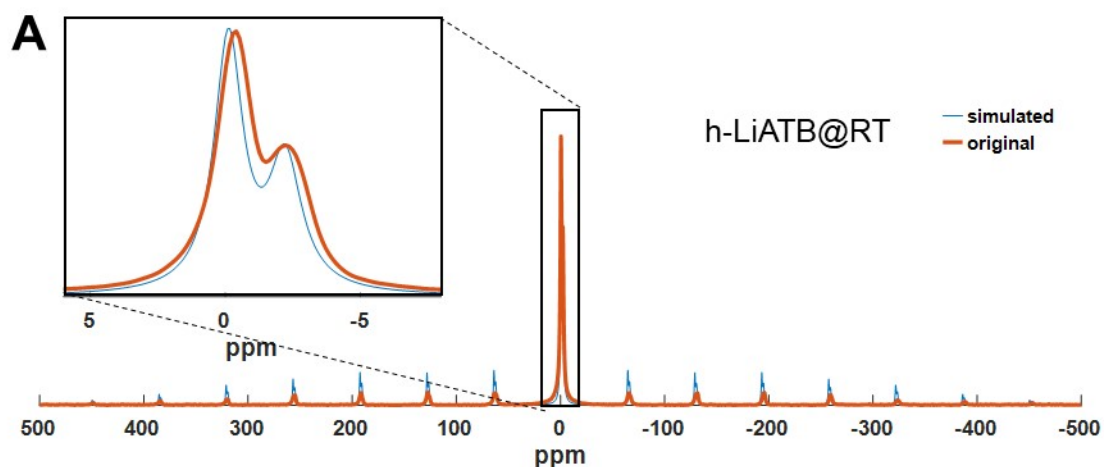


Fig. S13. Measured and simulated ⁷Li NMR spectra of h-LiTB@RT (A), h-LiTB@300 (B) and m-LiTb@500 (C) samples.

Table S5. Estimated quadrupole coupling constants and asymmetry parameters from simulated spinning sideband patterns using the SIMPSON software.

| sample | Shift / ppm | Cq / kHz | η |
|-------------|-------------|----------|--------|
| h-LiATB@RT | -0.46 | 150 | 0.5 |
| | -2.20 | 120 | 0.3 |
| h-LiATB@300 | -0.51 | 160 | 0.7 |
| | -2.57 | 90 | 0.7 |
| m-LiT@500 | -0.50 | 30 | 0.2 |
| | -1.44 | 110 | 0.7 |
| | -2.16 | 60 | 0.1 |